Scientific Computation of Two–Phase Ferrofluid Flows

Gareth Johnson

Faculty Adviser: Prof. Ricardo Nochetto

University of Maryland
AMSC 663: Advanced Scientific Computing I
Supported by Johns Hopkins University Applied Physics Lab

October 2, 2018

What is a Ferrofluid?

A ferrofluid is a colloid of nanoscale ferromagnetic particles suspended in a carrier fluid such as oil, water, or an organic solvent.

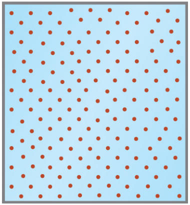

Ferrofluids become magnetized when under the effect of a magnetic field.

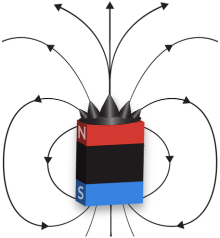

Applications

- Initially created to pump rocket fuel once a spacecraft entered a weightless environment.
- Commercial applications:
  - Vibration damping
  - Sensors
  - Acoustics
- Recent research areas:
  - Magnetic drug targeting
  - Adaptive deformable mirrors

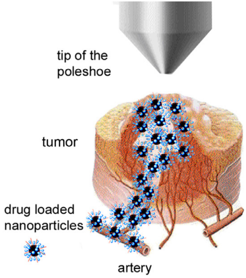

Previous Works

- Analytic works:
  - There are two well established PDE models which mathematically describe the behavior of a ferrofluid under the effects of a magnetic field.
    - The Rosensweig model
    - The Shliomis model
  - Existence of global weak solutions and local existence of strong solutions for both models are recent results [2, 3, 4, 5].
  - Issue: There is not an established PDE model which describes two–phase ferrofluid flows.
- Numerical works:
  - Stationary phenomena: Tobiska and collaborators investigated the free surface of ferrofluids using a sharp interface approach.
  - Non–stationary phenomena: Using a Volume of Fluid method
    - the field induced motion of a ferrofluid droplet was investigated [1],
    - the formation of ferrofluid droplets was investigated [11].
  - Issue:The above techniques numerical implementations, stability, and convergence were not explored.

PDE Model for Two–Phase Ferrofluid Flow

- Dr. Nochetto and collaborators developed a model for two–phase ferrofluid flows and devised an energy stable numerical scheme [12].
- The model was not derived, but instead was assembled.
- Important results from [12]:
  - Proved an energy law for the PDE model.
  - Proved the numerical scheme was energy stable and the existence of a local solution.
  - For an even simpler model, they proved stability, convergence, and the existence of solutions.

Modeling a Two–Phase Fluid

- In order to track both fluids, a diffuse interface is used.
- The phase variable θ is introduced, which takes values in $[-1, 1]$.
- The evolution of θ is given by a modified Cahn–Hilliard equation:

$$\begin{cases} \theta_t + \operatorname{div}(\mathbf{u}\theta) + \gamma\Delta\psi = 0 & \text{in } \Omega \\ \psi - \epsilon\Delta\theta + \frac{1}{\epsilon} f(\theta) = 0 & \text{in } \Omega \\ \partial_\eta\theta = \partial_\eta\psi = 0 & \text{on } \Gamma, \end{cases}$$

where

- $0 < \epsilon << 1$ is related to the interface thickness,
- $\gamma > 0$ is the constant mobility,
- ψ is the chemical potential,
- $f(\theta)$ is the truncated double well potential.

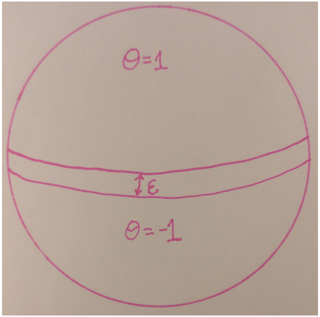

Modeling of the Magnetic Field

- Instead of using the magnetostatics equations, a simplified approach was used.
- Define the magnetic field by

$$\mathbf{h} := \mathbf{h}_a + \mathbf{h}_d,$$

  where
  - $\mathbf{h}_a$ – smooth harmonic (curl–free and div–free) applied magnetizing field,
  - $\mathbf{h}_d$ – demagnetizing field.
- Then the magnetic field is induced via the scalar potential φ by

$$\mathbf{h} = \nabla\varphi,$$

  along with,

$$-\Delta\varphi = \mathrm{div}(\mathbf{m} - \mathbf{h}_a) \quad \text{in } \Omega, \qquad \partial_\eta\varphi = (\mathbf{h}_a - \mathbf{m}) \cdot \eta \quad \text{on } \Gamma.$$

Modeling of Ferrohydrodynamics

- A simplified version of Shliomis model is used, which couples an advection–reaction equation for the magnetization $\mathbf{m}$:

$$\mathbf{m}_t + (\mathbf{u} \cdot \nabla)\mathbf{m} = -\frac{1}{\mathscr{T}}(\mathbf{m} - \varkappa_\theta \mathbf{h}),$$

  with the Navier–Stokes equations of incompressible fluids for the velocity–pressure pair $(\mathbf{u}, p)$:

$$\mathbf{u}_t + (\mathbf{u} \cdot \nabla)\mathbf{u} - \operatorname{div}(\nu_\theta \mathbf{T}(\mathbf{u})) + \nabla p = \mu_0(\mathbf{m} \cdot \nabla)\mathbf{h} + \frac{\lambda}{\epsilon}\theta\nabla\psi,$$

$$\operatorname{div}\mathbf{u} = 0,$$

  where
  - $\mathscr{T}$ is the relaxation time of the ferrofluid,
  - $\varkappa_\theta$ is the magnetic susceptibility of the phase variable,
  - ν_θ is the viscosity of the phase variable,
  - μ_0 is the constitutive parameter related to the Kelvin force,
  - $\frac{\lambda}{\epsilon}\theta\nabla\psi$ is the capillary force.
- This is supplemented with a no–slip condition on the boundary:

$$\mathbf{u} = 0 \quad \text{on } \Gamma.$$

- The model reads: Consider a bounded convex polygon/polyhedron domain $\Omega \subset \mathbb{R}^d$ ($d = 2$ or 3) with boundary Γ. The evolution of the system is given by the following set of equations in strong form in Ω

$$\theta_t + \mathrm{div}(\mathbf{u}\theta) + \gamma\Delta\psi = 0, \tag{1a}$$

$$\psi - \epsilon\Delta\theta + \frac{1}{\epsilon}f(\theta) = 0, \tag{1b}$$

$$\mathbf{m}_t + (\mathbf{u}\cdot\nabla)\mathbf{m} = -\frac{1}{\mathscr{T}}(\mathbf{m} - \varkappa_\theta \mathbf{h}), \tag{1c}$$

$$-\Delta\varphi = \mathrm{div}(\mathbf{m} - \mathbf{h}_a), \tag{1d}$$

$$\mathbf{u}_t + (\mathbf{u}\cdot\nabla)\mathbf{u} - \mathrm{div}(\nu_\theta \mathbf{T}(\mathbf{u})) + \nabla p = \mu_0(\mathbf{m}\cdot\nabla)\mathbf{h} + \frac{\lambda}{\epsilon}\theta\nabla\psi, \tag{1e}$$

$$\mathrm{div}\mathbf{u} = 0, \tag{1f}$$

for every $t \in [0, t_F]$, where $\mathbf{T}(\mathbf{u}) = \frac{1}{2}(\nabla\mathbf{u} + \nabla\mathbf{u}^T)$ denotes the symmetric gradient and $\mathbf{h} = \nabla\varphi$. The system (1) is supplemented with the boundary conditions

$$\partial_\eta\theta = \partial_\eta\psi = 0, \quad \mathbf{u} = 0, \quad \text{and} \quad \partial_\eta\varphi = (\mathbf{h}_a - \mathbf{m})\cdot\eta \quad \text{on } \Gamma. \tag{2}$$

Define the backward difference operator $\delta f^k = f^k - f^{k-1}$.

For given smooth initial data $\{\Theta^0, \mathbf{M}^0, \mathbf{U}^0\}$ and timestep τ, compute $\{\Theta^k, \Psi^k, \mathbf{M}^k, \Phi^k, \mathbf{U}^k, P^k\} \in \mathbb{G}_h \times \mathbb{Y}_h \times \mathbb{M}_h \times \mathbb{X}_h \times \mathbb{U}_h \times \mathbb{P}_h$ for every $k \in \{1, ..., K\}$ that solves

$$\left(\frac{\delta\Theta^k}{\tau}, \Lambda\right) - (\mathbf{U}^k\Theta^{k-1}, \nabla\Lambda) - \gamma(\nabla\Psi^k, \nabla\Lambda) = 0, \tag{3a}$$

$$(\Psi^k, \Upsilon) + \epsilon(\nabla\Theta^k, \nabla\Upsilon) + \frac{1}{\epsilon}(f(\Theta^{k-1}), \Upsilon) + \frac{1}{\eta}(\delta\Theta^k, \Upsilon) = 0, \tag{3b}$$

$$\left(\frac{\delta\mathbf{M}^k}{\tau}, \mathbf{Z}\right) - \mathcal{B}_h^m(\mathbf{U}^k, \mathbf{Z}, \mathbf{M}^k) + \frac{1}{\mathscr{T}}(\mathbf{M}^k, \mathbf{Z}) = \frac{1}{\mathscr{T}}(\varkappa_\theta\mathbf{H}^k, \mathbf{Z}), \tag{3c}$$

$$(\nabla\Phi^k, \nabla X) = (\mathbf{h}_a^k - \mathbf{M}^k, \nabla X), \tag{3d}$$

$$\begin{aligned}\left(\frac{\delta\mathbf{U}^k}{\tau}, \mathbf{V}\right) + \mathcal{B}_h(\mathbf{U}^{k-1}, \mathbf{U}^k, \mathbf{V}) + (\nu_\theta\mathbf{T}(\mathbf{U}^k), \mathbf{T}(\mathbf{V})) - (P^k, \mathrm{div}\mathbf{V}) &= \mu_0\mathcal{B}_h^m(\mathbf{V}, \mathbf{H}^k, \mathbf{M}^k) \\ &\quad + \frac{\lambda}{\epsilon}(\Theta^{k-1}\nabla\Psi^k, \mathbf{V}),\end{aligned} \tag{3e}$$

$$(Q, \mathrm{div}\mathbf{U}^k) = 0. \tag{3f}$$

Project Goals

1) Finite Element Code: Develop a finite element code to solve two–phase ferrofluid flows using the numerical scheme (3). This code will be written in a "dimensional–less" way, explained later, so that the code can be easily transitioned from 2d to 3d.
2) Solvers: In order to solve (3), three different solvers are required.
3) Scientific Questions: Investigate the structure of the velocity field of the fluid flow and the and magnetic field around the spike deformation of the ferrofluid for both the Rosenswieg instability and the ferrofluid hedgehog configuration in 2d.

If time permits, the following extensions of the project will be explored:

4) Parallelization: Implement parallel adaptive mesh refinement/coarsening.
5) Ferrofluid Droplets: Investigate if the model can accurately capture various effects of ferrofluid droplets, such as the coalescence of droplets [9] and the equilibrium shape of droplets under a uniform magnetic field [13].

Finite Element Code:

1) Write codes to handle the generation of the finite element spaces given in [12].
2) Write codes to handle the generation and adaptive refinement/coarsening of the mesh.
3) Write a code to handle the generation of the matrices, which will combine information from the mesh and the finite elements.
4) Write codes that solve each of the three subsystems, namely the Cahn–Hilliard system (3a)–(3b), the magnetization system (3c)–(3d), and the Navier–Stokes system (3e)–(3f).
5) Write a code to solve the full system (3) at each time step using a Picard–like iteration.
6) Write a code to handle the generation of the magnetic potential, given the locations of each magnetic dipole.
7) Include functionality for the numerical simulation to be restarted from the last completed iteration.

Numerical Investigation:

- Generate and analyze contour and vector plots of the velocity and magnetic field for the three experiments performed in [12].

Discretization of the Numerical Scheme

Recall (3):

$$
\begin{aligned}
\left(\frac{\delta\Theta^k}{\tau}, \Lambda\right) - (\mathbf{U}^k\Theta^{k-1}, \nabla\Lambda) - \gamma(\nabla\Psi^k, \nabla\Lambda) &= 0, \\
(\Psi^k, \Upsilon) + \epsilon(\nabla\Theta^k, \nabla\Upsilon) + \frac{1}{\epsilon}(f(\Theta^{k-1}), \Upsilon) + \frac{1}{\eta}(\delta\Theta^k, \Upsilon) &= 0, \\
\left(\frac{\delta\mathbf{M}^k}{\tau}, \mathbf{Z}\right) - \mathcal{B}_h^m(\mathbf{U}^k, \mathbf{Z}, \mathbf{M}^k) + \frac{1}{\mathscr{T}}(\mathbf{M}^k, \mathbf{Z}) &= \frac{1}{\mathscr{T}}(\varkappa_\theta\mathbf{H}^k, \mathbf{Z}), \\
(\nabla\Phi^k, \nabla X) &= (\mathbf{h}_a^k - \mathbf{M}^k, \nabla X), \\
\left(\frac{\delta\mathbf{U}^k}{\tau}, \mathbf{V}\right) + \mathcal{B}_h(\mathbf{U}^{k-1}, \mathbf{U}^k, \mathbf{V}) + (\nu_\theta\mathbf{T}(\mathbf{U}^k), \mathbf{T}(\mathbf{V})) - (P^k, \mathrm{div}\mathbf{V}) &= \mu_0\mathcal{B}_h^m(\mathbf{V}, \mathbf{H}^k, \mathbf{M}^k) \\
&\quad + \frac{\lambda}{\epsilon}(\Theta^{k-1}\nabla\Psi^k, \mathbf{V}), \\
(Q, \mathrm{div}\mathbf{U}^k) &= 0.
\end{aligned}
$$

- Time Discretization: Backward Euler is used.
- Space Discretization: A mix of Continuous and Discontinuous Galerkin is used, approximating the spaces with polynomials of degree 2 in each variable.
  - Continuous: Cahn–Hilliard and Navier Stokes equations.
  - Discontinuous: Magnetization equations.

Fixed Point Solver

- A Picard–like iteration is used.
- Utilizes the "lagging" of the velocity $\mathbf{U}$ to solve each subsystem.
- Iterates until a fixed point for $\mathbf{U}^k$ is reached.

Given $\mathbf{U}^{k-1}$

1) Compute Θ^k and Ψ^k substituting $\mathbf{U}^{k-1}$ for $\mathbf{U}^k$.
2) Next compute $\mathbf{M}^k$ and Φ^k using (Θ^k, Ψ^k) from the previous iteration and substituting $\mathbf{U}^{k-1}$ for $\mathbf{U}^k$.
3) Finally, compute $\mathbf{U}^k$ and P^k using $(\Theta^k, \Psi^k, \mathbf{M}^k, \Phi^k)$ from the previous two iterations.
4) Repeat steps 1-3 using $\mathbf{U}^k$ from the previous iteration as input until $\mathbf{U}^k$ does not change between iterations.

Subsystem Solvers

Cahn–Hilliard system (3a)–(3b):

- Linearized using convex–concave splitting:

$$f(\Theta^k) \to f(\Theta^{k-1}) + \eta\delta\Theta^k, \qquad \text{where } \eta \le \big(\max_\theta f'(\theta)\big)^{-1}.$$

- The resulting system is linear but non–symmetric.
- Solved using GMRES preconditioned with algebraic multigrid.

Magnetization system (3c)–(3d):

- Equation (3c) is mass dominated and non–symmetric.
- Solved using BiCGstab.
- Equation (3d) is a Laplacian, which is symmetric.
- Solved using CG preconditioned with algebraic multigrid.

Navier–Stokes system (3e)–(3f):

- It is a non–symmetric saddle point problem.
- Solved using GMRES with a block preconditioner.
- Will explore preconditioners presented in Elman's book [8].

Adaptive Mesh Refinement/Coarsening

- In order to resolve the interface, we need $0 < \epsilon << 1$.
- This requires the mesh to be highly dense near the interface.
- If a uniform meshsize h is used, this would lead to very large linear systems.
- To overcome this, we will use adaptive mesh refinement/coarsening.

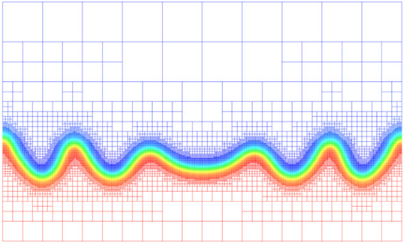

- The adaptive mesh refinement/coarsening will use the simplest element indicator η_T:

$$\eta_T^2 = h_T \int_{\partial T} \left| \left[\left[\frac{\partial \Theta}{\partial \eta} \right]\right] \right|^2 dS \quad \forall T \in \mathcal{T}_h.$$

Generation of the Magnetic Field

Define the magnetic dipole ϕ_s by

$$\phi_s(\mathbf{x}) = \frac{\mathbf{d} \cdot (\mathbf{x}_s - \mathbf{x})}{|\mathbf{x}_s - \mathbf{x}|},$$

where $|\mathbf{d}| = 1$ and $\mathbf{d}, \mathbf{x}_s, \mathbf{x} \in \mathbb{R}^2$. Then the applied magnetizing field $\mathbf{h}_a$ is given by

$$\mathbf{h}_a = \sum_s \alpha_s(t) \nabla \phi_s,$$

where $\alpha_s(t)$ is the intensity of each dipole.

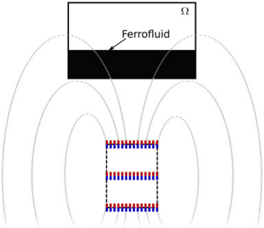

Target Platform

Hardware:

- A Linux desktop system.
- Using desktop owned by Dr. Nochetto with a Intel Xeon CPU with 24 cores and 68 GB of ram

Software:

- Developed in C++.
- The code will utilize the deal.II library [6, 7]. The library provides functionality to
  - create meshes,
  - generate finite elements,
  - aid in adaptive mesh refinement/coarsening,
  - solve linear algebra systems with preconditioners.

Distribution:

- Source code and user guide will be hosted on Github.

Validation Methods

Generated Solutions:

- Each of the three subsystems will be verified using a generated solution.
- Simple Example: For $u = \sin(x)$ to be a solution to

$$u' + u = 0,$$

  the forcing $f(x) = \sin(x) + \cos(x)$ will be added to the RHS.

Mesh Verification:

- Visually will verify input mesh.
- Adaptive mesh refinement/coarsening verified using a simple mesh with assigned error values.

Verification Methods (continued)

Comparison with prior works:

Uniform Magnetic Field

Non–uniform magnetic field $\mathbf{h} := \mathbf{h}_a + \mathbf{h}_d$

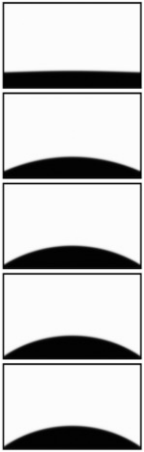

Non–uniform magnetic field $\mathbf{h} := \mathbf{h}_a$

Figure References

- Slide 1:
  - https://www.researchgate.net/profile/Vikram_Raghavan2/post/What_is_the_effect_of_magnetic_field_on_alignment_of_ferro_fluid_droplet/attachment/59d622166cda7b8083a1b9a2/AS%3A273810673078272%401442292959057/download/Effect+of+Magnetic+field.jpg
  - https://ksr-ugc.imgix.net/assets/003/310/641/f0ef73d1fd99f6aa5d96872168478df4_original.png?v=1424378871&w=680&fit=max&auto=format&lossless=true&s=c183d857603c12de82a71f3139283d9e
  - https://opentextbc.ca/chemistry/wp-content/uploads/sites/150/2016/05/CNX_Che_11_05_Colloid.jpg
- Slide 2: [10]
- Slide 15: [12]
- Slide 16: [12]
- Slide 18: [12]

References I

S. Afkhami, Y. Renardy, M. Renardy, J. S. Riffle, and T. St Pierre, *Field-induced motion of ferrofluid droplets through immiscible viscous media*, Journal of Fluid Mechanics, 610 (2008), p. 363–380.

Y. Amirat and K. Hamdache, *Global weak solutions to a ferrofluid flow model*, Mathematical Methods in the Applied Sciences, 31 (2007), pp. 123–151.

———, *Strong solutions to the equations of a ferrofluid flow model*, Journal of Mathematical Analysis and Applications, 353 (2009), pp. 271 – 294.

———, *Unique solvability of equations of motion for ferrofluids*, Nonlinear Analysis: Theory, Methods & Applications, 73 (2010), pp. 471 – 494.

Y. Amirat, K. Hamdache, and F. Murat, *Global weak solutions to equations of motion for magnetic fluids*, Journal of Mathematical Fluid Mechanics, 10 (2008), pp. 326–351.

W. Bangerth, C. Burstedde, T. Heister, and M. Kronbichler, *Algorithms and data structures for massively parallel generic adaptive finite element codes*, ACM Trans. Math. Softw., 38 (2012), pp. 14:1–14:28.

W. Bangerth, T. Heister, and G. Kanschat, *Deal.ii differential equations analysis library, technical reference*.

H. Elman, D. Silvester, and A. Wathen, *Finite Elements and Fast Iterative Solvers with Applications in Incompressible Fluid Dynamics*, Oxford University Press, 2005.

A. Ghaffari and S. H. Hashemabadi, *Parameter study and cfd analysis of head on collision and dynamic behavior of two colliding ferrofluid droplets*, Smart Materials and Structures, 26 (2017).

References II

C. Janko, S. Dürr, L. E. Munoz, S. Lyer, R. Chaurio, R. Tietze, S. v. Löhneysen, C. Schorn, M. Herrmann, and C. Alexiou, *Magnetic drug targeting reduces the chemotherapeutic burden on circulating leukocytes*, International Journal of Molecular Sciences, 14 (2013), pp. 7341–7355.

J. Liu, S.-H. Tan, Y. F. Yap, M. Y. Ng, and N.-T. Nguyen, *Numerical and experimental investigations of the formation process of ferrofluid droplets*, Microfluidics and Nanofluidics, 11 (2011), pp. 177–187.

R. H. Nochetto, A. J. Saldago, and I. Tomas, *A diffuse interface model for two-phase ferrofluid flows*, Computer Methods in Applied Mechanics and Engineering, 309 (2016), pp. 497–531.

P. Rowghanian, C. D. Meinhart, and O. Campàs, *Dynamics of ferrofluid drop deformations under spatially uniform magnetic fields*, Journal of Fluid Mechanics, 802 (2016), pp. 245–262.